

Widely tunable Yb:KYW laser with a volume Bragg grating

Björn Jacobsson, Jonas E. Hellström, Valdas Pasiskevicius and Fredrik Laurell

Laser physics, KTH – Royal Institute of Technology, 106 91 Stockholm, Sweden

bj@laserphysics.kth.se

Abstract: We demonstrate a narrowband, continuously tunable Yb:KYW laser locked by a volume Bragg grating at oblique incidence in a retroreflector configuration. The tuning range was 997 nm to 1050 nm (15 THz) with bandwidth < 0.1 nm and a maximum output power of 4.7 W. In a high-quality beam with $M^2 < 1.3$, the maximum output power was 1.7 W. We also demonstrate 3 W output power at 1064 nm from the same Yb:KYW laser with the grating at normal incidence.

©2007 Optical Society of America

OCIS codes: (050.7330) Volume holographic gratings; (140.5680) Rare earth and transition metal solid-state lasers; (140.3600) Lasers, tunable.

References and links

1. J. Liu, U. Griebner, V. Petrov, H. Zhang, J. Zhang, and J. Wang, "Efficient continuous-wave and Q-switched operation of a diode-pumped Yb:KLu(WO₄)₂ laser with self-Raman conversion," *Opt. Lett.* **30** 2427-2429 (2005).
2. A. Brenier, "A new evaluation of Yb³⁺-doped crystals for laser application," *J. Lumin.* **92** 199-204 (2001).
3. J. E. Hellström, S. Bjurshagen, V. Pasiskevicius, J. Liu, V. Petrov, and U. Griebner, "Efficient Yb:KGW lasers end-pumped by high-power diode bars," *Appl. Phys. B* **83** 235-239 (2006).
4. F. Druon, S. Chénais, F. Balembos, P. Georges, A. Brun, A. Courjaud, C. Hönninger, F. Salin, M. Zavelani-Rossi, F. Augé, J. P. Chambaret, A. Aron, F. Mougel, G. Aka and D. Vivien, "High-power diode-pumped Yb:GdCOB laser: from continuous-wave to femtosecond regime," *Opt. Mat.*, **19** 73-80 (2002).
5. W. Li, Q. Hao, H. Zhai, H. Zeng, W. Lu, G. Zhao, C. Yan, L. Su and Jun Xu, "Low-threshold and continuously tunable Yb:Gd₂SiO₅ laser," *Appl. Phys. Lett.* **89** 101125-1-3 (2006).
6. M. Jacquemet, F. Druon, F. Balembos and P. Georges, "Single-frequency operation of diode-pumped Yb:KYW at 1003.4 nm and 501.7 nm by intracavity second harmonic generation," *Appl. Phys. B* **85** 69-72 (2006).
7. F. Havermeier, W. Liu, C. Moser, D. Psaltis, and G. J. Steckman, "Volume holographic grating-based continuously tunable optical filter," *Opt. Eng.* **43** 2017-2021 (2004).
8. O. Efimov, L. Glebov, L. Glebova, K. Richardson and V. Smirnov, "High-efficiency Bragg gratings in photothermorefractive glass," *Appl. Opt.* **38** 619-627 (1999).
9. B. Volodin, S. Dolgy, E. Melnik, E. Downs, J. Shaw and V. Ban, "Wavelength stabilization and spectrum narrowing of high-power multimode laser diodes and arrays by use of volume Bragg grating," *Opt. Lett.* **29** 1891-1893 (2004).
10. B. Jacobsson, V. Pasiskevicius, and F. Laurell, "Tunable single-longitudinal-mode ErYb:glass laser locked by a bulk glass Bragg grating," *Opt. Lett.* **31** 1663-1665 (2006).
11. T. Chung, A. Rapaport, V. Smirnov, L. B. Glebov, M. C. Richardson, and M. Bass, "Solid-state laser spectral narrowing using a volumetric photothermal refractive Bragg grating cavity mirror," *Opt. Lett.* **31** 229-231 (2006).
12. B. Jacobsson, V. Pasiskevicius, and F. Laurell, "Single-longitudinal-mode Nd-laser with a Bragg-grating Fabry-Perot cavity," *Opt. Express* **20** 9284-9292 (2006).
13. B. Jacobsson, M. Tiihonen, V. Pasiskevicius, and F. Laurell, "Narrowband bulk bragg grating optical parametric oscillator," *Opt. Lett.* **30** 2281-2283 (2005).
14. B. Jacobsson, J. E. Hellström, V. Pasiskevicius, and F. Laurell, "Transversal mode transformation in reflective volume Bragg gratings, theory and experiments," *Advanced Solid-State Photonics* (2007).
15. J. E. Hellström, S. Bjurshagen, V. Pasiskevicius: "Laser performance and thermal lensing in high-power diode pumped Yb:KGW with athermal orientation," *Appl. Phys. B* **83** 55-59 (2006).

1. Introduction

Ytterbium-doped lasers have met a lot of interest due to their attractive properties such as a low quantum defect, a wide gain spectrum and an absorption suitable for diode pumping. Among the various host materials that have been investigated, the double-tungstate crystals such as $\text{KGd}(\text{WO}_4)_2$ (KGW), $\text{KY}(\text{WO}_4)_2$ (KYW) and $\text{KLu}(\text{WO}_4)_2$ (KLuW), have shown the highest efficiencies [1, 2], while having good mechanical properties. This has led to the realisation of compact lasers with high continuous wave power [3]. If these lasers are combined with proper spectral control, the wide gain bandwidth should yield an efficient tunable laser source in the 1 μm region. Such a laser source has many applications, e.g. in spectroscopy and material characterisation.

Earlier, tuning of Yb-doped double tungstates has been demonstrated by insertion of an intra-cavity etalon [3]. However, due to the limited free spectral range of the etalon, the tuning range was only 1021-1041 nm. In other host materials, wide tunability ranges have been achieved by use of intracavity prisms [4, 5]. However, the dispersion provided by a single prism is not sufficient for narrowband filtering so multiple prism arrangements are needed which introduces additional losses into the cavity. Furthermore, for the case of pumping at 980 nm, there is to our knowledge only one report, where the wavelength has been tuned below 1010 nm with power levels above 10 mW [6]. In those experiments, the wavelength was controlled by a combination of a wavelength selective dielectric coating and an etalon. Apart from Yb-doped lasers, Ti:sapphire lasers are an obvious alternative as tunable laser sources in the 1 μm region. However, they present low efficiencies since they need optical pumping in the green part of the spectrum and have a low emission cross section above 1 μm , which considerably increases size and cost of the system.

In this work our aim is to demonstrate an efficient and widely tunable laser source operating around 1 μm , which is based on Yb:KYW as the gain medium. We employ a volume Bragg grating at oblique incidence as the wavelength selective component. In this way we achieve a narrow spectral bandwidth in combination with a wide tuning range – the widest so far in this material. By a novel design with an intracavity retroreflector arrangement incorporating the volume Bragg grating [7], we obtain simple tuning of the laser by adjusting only one degree of freedom. In comparison with the other tuning methods discussed above, volume Bragg gratings in a single element provide a better wavelength selectivity than prisms and, unlike the multiple peaks in etalons, give a minimum cavity loss at a single wavelength only.

Volume Bragg gratings consist of photosensitive glass with a sinusoidal refractive index modulation throughout the volume [8]. These devices enable a high peak reflection combined with a very small reflection bandwidth on the sub-nanometer scale. Previously, volume Bragg gratings have been used to lock the wavelength of high-power diode lasers [9], as well as various solid-state lasers: ErYb:glass [10], Ti:sapphire [11], Cr:LiSAF [11] and Nd:GdVO₄ [12]. However, in these cases the laser was locked to a single wavelength and could not be tuned more than permitted by temperature tuning of the Bragg peak, i.e. some nanometers at most.

Extensive tuning of the reflected wavelength from a Bragg grating can be achieved by turning the grating. The reflected wavelength, λ , is tuned with the (internal) angle of incidence θ , according to $\lambda = \lambda_0 \cos\theta$, where λ_0 is the wavelength at a normal incidence. This approach was used to control the wavelength of an optical parametric oscillator in Ref. [13]. Angle tuning of the Bragg reflectivity maximum is also employed in the current work. However, the oblique propagation of an optical beam in a volume Bragg grating has some important consequences such as dependence of the reflectivity on the beam size and a filtering action on the spatial distribution of the beams, which have to be taken into consideration in designing the tuning element. These issues have been reported in Ref. [14], and will be discussed below.

2. Experimental setup

Throughout this work, a 5 at.% Yb:KYW laser crystal was used. The dimensions were $3 \times 3 \times 3 \text{ mm}^3$ and the crystal was cut for propagation along the dielectric axis N_p , i.e. the crystallographic axis b . Both end facets of the crystal were AR-coated. Two side facets of the crystal were covered by In-foil and pressed into a water-cooled copper holder. The largest absorption cross-section in monoclinic double tungstates such as Yb:KYW is for light polarized parallel to the N_m dielectric axis and thus there are some benefits in using polarized pump light [3]. Consequently we employed a diode bar (Limo GmbH) as a pump source, consisting of 19 single emitters at a wavelength of 980 nm with a full width at half maximum (FWHM) spectral width of 2.4 nm as a pump source and 95% nominal linear polarization. Due to the quasi-three-level nature of the gain medium high pumping intensity and good mode-matching between the cavity and the pump are required in order to reduce reabsorption losses. This is especially important for short-wavelength operation of this laser, where the absorption cross-section is high. The pump beam was focussed through a flat input coupler mirror to a focal spot with radii ($1/e^2$) of $100 \mu\text{m} \times 80 \mu\text{m}$ in the crystal. The focus was Gaussian along the $80 \mu\text{m}$ -direction, and close to top-hat along the other direction. The input coupler was coated for high-reflectivity (HR >99.9%) in the 1020-1200 nm wavelength region, decreasing from R=99.5% at 1010 nm to about R=95% at 1000 nm and R=75% at 995 nm, as well as coated for high transmission (>99%) at the pump wavelength of 980 nm. The complete set of pumping optics transmitted a maximum pump power of 19.3 W onto the laser crystal, of which around 90 % was absorbed under lasing conditions.

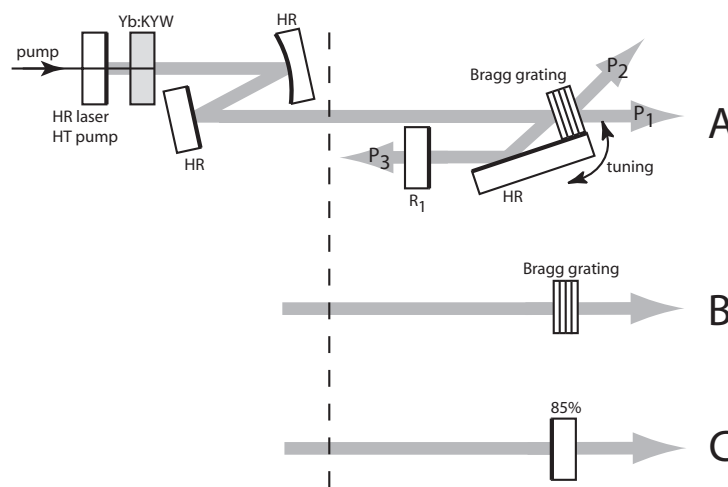


Fig. 1. Laser setups A, B and C.

The wavelength locking and tuning of the laser were accomplished by means of a reflective volume Bragg grating in a retroreflector design, as can be seen in Fig. 1(A). The retroreflector in this work was constituted by the Bragg grating together with a flat dielectric mirror, specified for HR between 1010 nm and 1050 nm for 63° to 77° angle of incidence, respectively. The grating was mounted perpendicular to the dielectric mirror, both on the same rotation stage. As is well known, a retroreflector arrangement redirects the output beam in the direction opposite to that of the incoming beam, regardless of exact angle of incidence onto the mirrors. By rotating the retroreflector around an axis at the crossing point of the two mirrors, the wavelength can be tuned without beam steering and with preserved cavity alignment. The Bragg grating (Ondax Inc.) had a peak reflectivity for plane waves at normal incidence of 97% at 1063.5 nm and a FWHM bandwidth of 0.55 nm. To avoid parasitic reflections from the facets, these were tilted by a few degrees with respect to the grating direction as well as AR-coated.

For the laser cavity design, three things have to be considered. First, since Yb is a three level laser system, the mode size in the Yb crystal must be small in order to get a large inversion and reduce reabsorption losses. The size is determined by the smallest possible spot of the pump. Second, since the thermal lens in Yb:KYW can have focal lengths as short as 30 mm for the highest pump power [15], the cavity should be at a stability maximum, to minimize the perturbing thermal effects to the cavity design. Third, the mode size on the volume Bragg grating should be as large as allowed by the grating aperture, in order to reduce the beam-distorting and reflectivity-lowering effects of oblique incidence of a finite size beam on a thick grating. This effect can be understood by considering the reduced acceptance angle of the grating with increased angle of incidence, which requires a large beam size with correspondingly small beam divergence.

The cavities we used are depicted in Fig. 1. To simplify the cavity as much as possible while fulfilling the requirements listed above, we chose to use a folded cavity as a basis, with a curved folding mirror. The 200 mm radius of curvature mirror imaged a small mode size of $\sim 80 \mu\text{m}$ in the Yb-crystal in one arm onto a large mode size of $\sim 300 \mu\text{m}$ on the Bragg grating in the other arm. The arm lengths and curved mirror power were chosen to maximize the cavity stability for no thermal lens in the Yb-crystal, resulting in a total cavity length of 470 mm. In order to minimize the astigmatism in the curved folding mirror, the angle of incidence was 3.5° . The retroreflector arm was completed by a flat mirror, R_1 , as depicted in Fig. 1(A). The reflectivity of R_1 was varied between HR, 95% and 85%. For the HR case, the cavity has two output beams, denoted by P_1 and P_2 , with one more added for the 95% and 85% case, denoted by P_3 .

In order to reach the longest possible wavelength of 1064 nm for our specific Bragg grating, we used it at normal incidence as shown in Fig. 1(B). Finally, for comparison, an ordinary flat output coupler of 85% reflectivity was used instead of the grating arrangements, see Fig. 1(C).

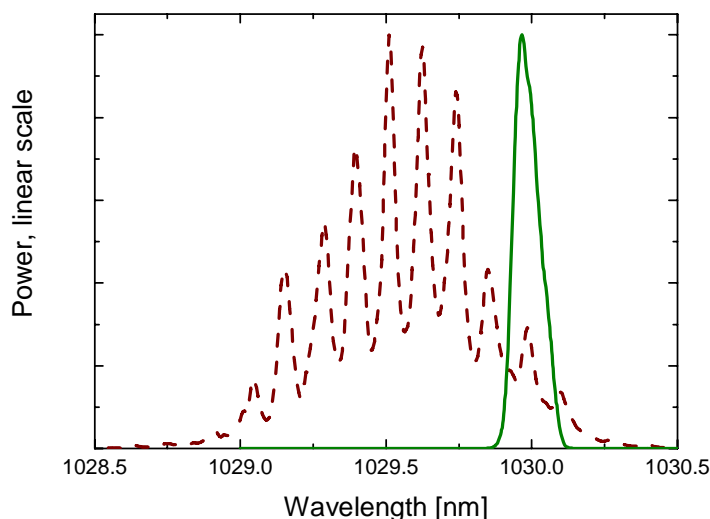


Fig. 2. Comparison between the spectra of the Bragg locked laser in cavity A (solid green) and of the free running laser in cavity C (dashed brown), both at 19 W pump power.

3. Results

The spectral discrimination properties of the volume Bragg grating retroreflector is demonstrated in Fig. 2, where the spectra of the laser cavities A and C are compared at full pump power, as measured with a grating based optical spectrum analyser. The Bragg-locked laser with the retroreflector design, cavity A, showed a spectral bandwidth of 0.1 nm and was temporally stable. Also for cavity B, a stable output with a spectral bandwidth $< 0.05 \text{ nm}$ was found. In comparison, the free running laser with no wavelength-selective element lased at

1029.6 nm, with a bandwidth of about 0.5 nm. This laser also showed a number of longitudinal mode clusters with a separation of ~ 0.12 nm, most likely caused by an etalon effect in one of the cavity elements. It should be noted that the longitudinal mode spacing for our cavities is about 1.3 pm and cannot be resolved in this spectrum.

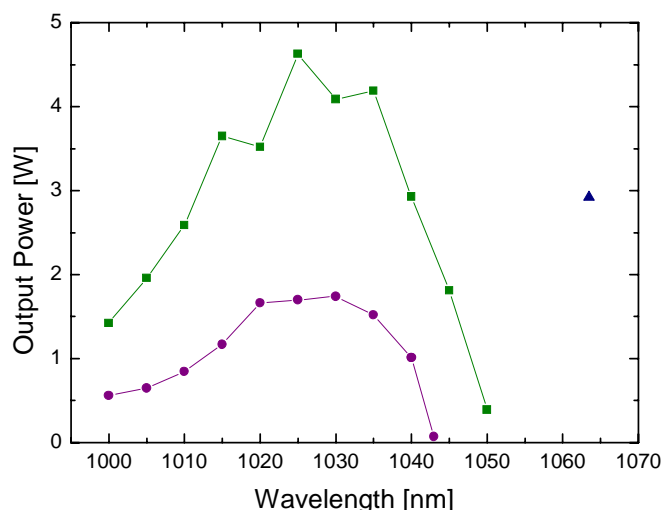


Fig. 3. Tunability of the Bragg locked laser in cavity A with respect to the total power P_1+P_2 using $R_1 = \text{HR}$ (green squares) and with respect to P_3 using $R_1 = 85\%$ (purple circles). The output power of cavity B is also shown (blue triangle). The pump power is 19 W.

The wavelength of the laser with the Bragg grating could easily be continuously tuned by rotating the retroreflector. Realignment of the cavity mirrors were not required throughout the tuning range. The output power as a function of wavelength for full pump power is displayed in Fig. 3 for two different output couplers, $R_1=\text{HR}$ or $R_1=85\%$. For $R_1=\text{HR}$, we show the total transmitted power through the grating in both output beams P_1 and P_2 . In this configuration, the laser wavelength could be tuned continuously between 997 nm and 1050 nm with a maximum output power reaching 4.5 W at 1025 nm. With an increased outcoupling $R_1=85\%$, the longest wavelength of the tunability range was limited to 1043 nm due to decreasing Yb:KYW gain at longer wavelengths. The longest wavelength generated was reached in cavity configuration B, where the grating was at normal incidence and the laser was locked to a wavelength of 1063.7 nm. As has been noted before [12], the wavelength shifted slightly with the laser power, from 1063.43 nm for a pump power of 7.7 W up to 1063.71 nm for a pump power of 19 W. This we attribute to heating of the grating, which causes a tuning of the peak by ~ 0.01 nm/K [9, 11, 13], in our case indicating a heating of 30 K.

The slope efficiencies and thresholds for different wavelengths using cavity A with the high reflectivity end mirror R_1 are shown in Fig. 4. Since the threshold depends on the total loss-gain balance, while the slope efficiency depends on the output coupling to the loss ratio, this figure gives some insight to the properties and limitations of the laser. For comparison, we also show a prediction of the threshold given by the measured absorption and emission cross sections of our crystal together with the outcoupling losses, as determined below. It can be seen that the shape of the experimental threshold curve is as expected from the variation of absorption, emission and outcoupling with wavelength. The slope efficiency curve indicates some additional losses at the shortest and longest wavelengths, since it drops rapidly despite the fairly constant output coupling. The limitation of our laser at longer wavelengths is simply that the beam does not fit on the broadband mirror part of the retroreflector for small incidence angles on the Bragg grating. At shorter wavelengths, the limiting factor is the incoupling mirror, with a reflectivity that drops sharply below 1000 nm, which prevents lasing.

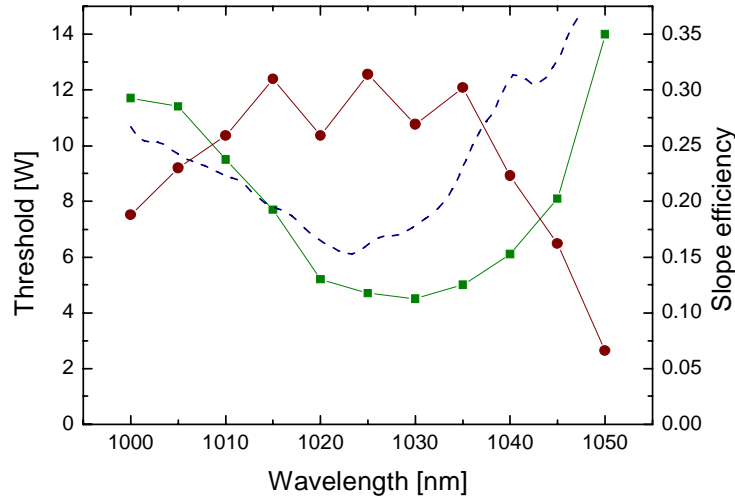


Fig. 4. Thresholds of incident pump power (green squares) and slope efficiencies (brown circles) of cavity A with respect to total power P_1+P_2 using $R_1 = HR$. The blue dashed line is the predicted threshold from absorption and emission cross section data together with mirror reflectivities.

As was discussed above, the reflectivity of the volume Bragg grating decreases with increasing incident angle. In order to estimate this effect, we measured the power P_1 transmitted through the grating and compared to the power P_3 transmitted by the output coupler R_1 . Two output couplers with $R_1=85\%$ and $R_1=95\%$ were compared, and the wavelength of the laser was tuned by rotating the retroreflector at maximum pump power. As can be seen from Fig. 5, the reflectivity of the grating is indeed decreasing with increasing incidence angle.

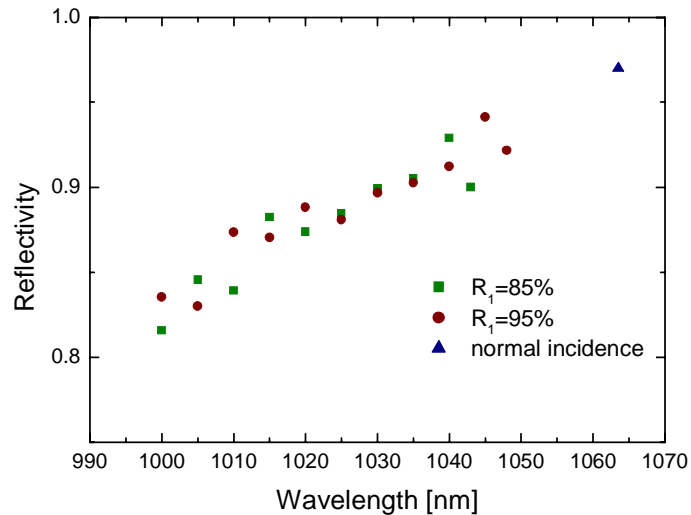


Fig. 5. Deduced volume Bragg grating reflectivities for different incidence angles and for two different output couplers at 19 W pump power. Shown is also the value at normal incidence.

The fact that the Bragg grating reflectivity is limited by how well the incident beam fits under the grating's acceptance angle, leads to a transversal mode selectivity, since higher order mode beams contain larger angles. This, together with the mode conversion properties of the grating for oblique incidence [14], results in low beam qualities of P_1 and P_2 in the

tangential plane. For the P_1 beam, M^2 in the tangential plane at maximum pump power ranged from 2 at 1045 nm to around 5 at 1030 nm and shorter wavelengths. In the sagittal plane, M^2 was below 1.8 for all wavelengths. Concerning P_2 , the situation was worse and the beam profile was heavily distorted in the tangential plane. In this direction M^2 was measured to be well above 30 for all wavelengths. Meanwhile, in the sagittal plane an $M^2 \sim 5$ was obtained. The reason for the worse M^2 of P_2 compared to P_1 could possibly be explained by a difference in the transverse field of the incident beams on the grating. Two things can contribute to this. First the reflected beam after the first passage in direction P_1 gets a slightly distorted transversal shape. Second, it is possible that the phase front might get distorted due to reflections off imperfect surfaces in between the first and second reflection in the Bragg grating. A second indication of this difference in transverse fields is the fact that for $R_1=HR$, on average the ratio of the power in P_1 to P_2 is about 40:60, which could be explained by the above mentioned higher grating transmission of higher order modes. It should also be noted, that this difference in reflectivity does not imply a non-reciprocity of the grating, since the beam going back in the P_2 direction is not the same as the one reflected from the P_1 -direction, but rather with a transverse distribution that has been inverted.

Contrary to this, the beam quality of the internal laser mode in cavity A was good in all experiments, as shown by the fact that all output beams from ordinary mirrors had an M^2 -value of around 1.3 in both the vertical and horizontal direction. Specifically, P_3 in cavity A with $R_1=85\%$ had an $M^2 < 1.3$ even at maximum pump power. When used at normal incidence as in cavity B, the Bragg grating also produced output beams of good quality, M^2 -values between 1.3 and 2.2. The slight increase in M^2 -value can be understood by a stronger thermal lens caused by the larger quantum defect. For comparison, the M^2 value of cavity C with an ordinary mirror output coupler was found to be about 1.3.

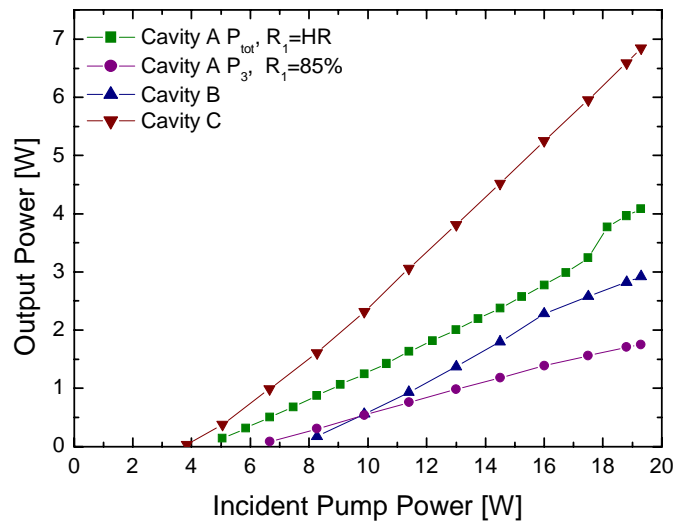


Fig. 6. Output power characteristics for cavity A and cavity C at 1030 nm, and for cavity B at 1064 nm.

The output powers of the different cavities are shown in Fig. 6. The polarization of the laser light in all cavities was parallel to the N_m dielectric axis, as expected due to the much higher emission cross section. In our setup, this gives p-polarisation incident on the Bragg grating. The reference, cavity C, with a dielectric mirror output coupling of 15% and operating at 1029 nm, showed a threshold of 3.8 W of incident pump power and a slope efficiency of 45%. This performance corresponds well to what has previously been demonstrated for the very similar Yb:KGW [3].

For cavity A with $R_1=HR$, tuned to 1030 nm, the output coupling losses through the Bragg grating per roundtrip is about 23%. Here the threshold was 4.5 W and the slope 27%. In

comparison with the reference cavity C, the threshold is slightly higher, and the slope efficiency is lower, resulting in less output power. We believe that the lower slope efficiency of the cavity with retroreflector is connected with a non-optimal overlap between the cavity transversal mode and the reflected transverse distribution of the grating. As shown in Fig. 3, a maximum total output power of 4 W was reached at 1030 nm, decreasing to about 1.5 W at 1000 nm and about 0.5 W at 1050 nm.

For the case of $R_1=85\%$ in cavity A, the total roundtrip output coupling was 36% at 1030 nm. Here, the threshold was reached at 6 W pump and the slope was 34%, with respect to the total output through beams P_1 , P_2 and P_3 (not shown in Fig. 6). As expected, with the increased outcoupling, the threshold is higher than for $R_1=HR$ and the slope is higher as well. As discussed above, it is beneficial in terms of beam quality to extract the power from the laser cavity through the output coupler R_1 , not through the Bragg grating at oblique incidence. Thus for the beam P_3 , the slope efficiency was 13% (see Fig. 6). The maximum output power P_3 at 1030 nm was 1.7 W, decreasing to 1 W at 1040 nm and 0.5 W at 1000 nm, as shown in Fig. 3.

Using the Bragg grating at normal incidence, as in cavity B, with an output coupling of 3%, we get a threshold of 7.5 W of incident pump power and a slope of 26%. As expected, the lower gain at 1063.7 nm gives a higher threshold than the reference, while the lower slope efficiency can be attributed to the lower output coupling. Still, a maximum output power of 3 W is achieved.

A positive side-effect of the output P_2 through the Bragg grating is that it acts as a spectrometer for the laser wavelength. Because the propagation direction of P_2 depends on the angle of the Bragg grating, it also depends on the wavelength. By simply measuring the angle of P_2 , the wavelength can thus easily be deduced.

4. Conclusion

We have demonstrated an Yb:KYW laser that is continuously tunable between 997 nm and 1050 nm, corresponding to 15 THz. The tuning was achieved with a reflective volume Bragg grating at an oblique angle in a retroreflector design. The laser bandwidth was 0.1 nm (30 GHz) and the maximum output power 4.5 W. In a single beam with $M^2 < 1.3$, we achieved a power of 1.7 W. Our experiments show that diode-pumped Yb:KYW locked by a volume Bragg grating can be a Ti:sapphire alternative above 1 μm wavelength.

To increase the laser power in a single beam of good beam quality, it would be beneficial to reduce the transmission through the Bragg grating. Here one needs to consider the effects of a finite beam incident at an oblique angle. Two approaches can be used, either having a grating with a larger aperture or simply increasing the plane wave reflectivity. An increase of the tuning range to longer wavelengths should be possible by simply replacing the grating for one with a peak shifted to correspondingly longer wavelengths.

Furthermore, we have demonstrated locking of an Yb:KYW laser at a fixed wavelength of 1063.7 nm with a volume Bragg grating at normal incidence. The maximum power was 3 W with a bandwidth of < 0.05 nm and an M^2 of 2. This shows that with this technique, it would be possible to lock an Yb:KYW laser to any fixed wavelength between at least 1000 nm and 1070 nm. More specifically, all Nd^{3+} wavelengths for the ${}^4F_{3/2} \rightarrow {}^4I_{11/2}$ transition can be reached. Replacing Nd for Yb is interesting due to the lower quantum defect, which potentially gives better laser performance.

Acknowledgments

We acknowledge financial support from the Göran Gustafsson foundation, the Carl Trygger Foundation as well as the EU project DT-CRYS.